Journal of Applied Mechanics and Technical Physics, Vol. 38, No. 6, 1997

DETERMINATION OF THE CONSTANTS OF SPALL-FRACTURE KINETICS OF MATERIALS USING EXPERIMENTAL DATA

A. V. Utkin

UDC 539.593

A large deal of experimental data on the character of spall fracture of various materials upon pulse tension have so far been obtained. In particular, for many metals, spall fracture has been shown to increase with an increase in the deformation velocity [1–3], which reflects the kinetic character of the fracture process. In this connection, it is of interest to study various methods of obtaining information on the kinetics of spall fracture directly from an analysis of experimental data. The author have shown such a possibility in [4, 5] where the effect of the initial fracture velocity on the formation of a spall pulse has been analyzed using the simplest models and the critical conditions of the formation of a minimum of a spall impact on the free-surface velocity profile have been found.

The goal of the present paper is to analyze the processes that occur in a medium subject to fracture when the compression pulse is reflected from a free surface and to study the possibility of obtaining information on the fracture velocity based on experimental data.

Formulation and Solution of the Problem. We study, in the acoustic approximation, the evolution of the compression pulse of arbitrary shape after its reflection from the free surface of a specimen which fractures under negative pressure. We assume that the fracture begins when tensile stresses reach the critical value P_{cr} and is characterized by the magnitude of the specific volume of pores v_p. The total specific volume of a medium is equal to the sum of v_p and the specific volume of the solid component v_s: $v = v_p + v_s$. In Lagrangian variables, the system of hydrodynamic equations, which is closed by the equations of kinetics and state, is of the form

$$\frac{\partial u}{\partial t} + \frac{\partial P}{\partial h} = 0, \quad \frac{\partial v}{\partial t} - \frac{\partial u}{\partial h} = 0, \quad P = \rho^2 c^2 \Big(\frac{1}{\rho} - v + v_p\Big), \quad \rho \frac{\partial v_p}{\partial t} = F(t, h), \tag{1}$$

where t is time, h is the Lagrangian coordinate, u is the mass velocity, and ρ and c are the initial density and the sound velocity, respectively. In the equation of state, the pressure is found as a function of the specific volume of the solid component in the equation of state. In addition, we assume that the rate of variation of the specific pore volume F can be expressed as the explicit function of coordinates and time.

Figure 1 shows the flow pattern in the plane t–h. In region 1, the interaction between the incident and reflected waves is absent; the dependence of the mass velocity and the pressure on the coordinates and time is determined by the shape of the initial compression pulse. For a simple wave, we have

$$u(h,t) = f(h - ct), \quad P(h,t) = \rho c u(h,t). \tag{2}$$

In region 3, the incident and reflected pulses ($h = 0$) interact with each other, which leads to the appearance of tensile stresses. Their absolute values do not exceed the critical one and, therefore, the medium does not fracture, and the solution, subject to the free-surface condition, is of the form

$$u(h,t) = f(h - ct) + f(-h - ct), \quad P(h,t) = \rho c(f(h - ct) - f(-h - ct)). \tag{3}$$

For $h = h_{cr}$ and $t = \tau_{cr} = -h_{cr}/c$, the pressures reaches the threshold P_{cr}, and the material fractures in region 2. The flow here is determined as a result of the solution of system (1) under the boundary conditions

Institute of Chemical Physics, Russian Academy of Sciences, Chernogolovka 142432. Translated from Prikladnaya Mekhanika i Tekhnicheskaya Fizika, Vol. 38, No. 6, pp. 157–166, November–December, 1997. Original article submitted April 9, 1996.

 0021-8944/97/3806-0952 $18.00

specified for $h = h_{cr}$ and $h \to -\infty$ and the initial conditions on the C_- characteristic passing through the coordinate origin.

We find the solution in region 2. For this, we exclude v and v_p from (1) and substitute the independent variables: $T = t + h/c$ and $x = h$.

After we have applied the Laplace transform with respect to the variable T to the resulting system of two partial equations, this system is transformed to the following system of ordinary differential equations:

$$\frac{d\hat{u}}{dx} + \frac{s}{c}\hat{u} + s\frac{\hat{P}}{\rho c^2} = \frac{1}{\rho c^2}J_+(0,x) + \hat{F}(s,x), \quad \frac{d\hat{P}}{dx} + \frac{s}{c}\hat{P} + \rho c\hat{u} = \frac{1}{c}J_+(0,x). \tag{4}$$

Here s is the Laplace variable, $\hat{u}$ and $\hat{P}$ are the Laplace images of the mass velocity and the pressure, and $\hat{F}(s,x)$ is the Laplace image of the fracture velocity. The initial values of u and P for $T \to +0$, which enter the Riemann J_+ invariant [6], are transferred to the right-hand side of Eq. (4). Therefore, there is no need to determine separately u and P on the right of the shock on the C_- characteristics, because they will be found directly from the solution of system (4). The value of the invariant is found from the continuity condition in the shock, depending on its magnitude in region 1. According to (2), we obtain $J_+(0,x) = 2\rho c f(2x)$.

The general solution in the fracture region, which does not increase exponentially for $x \to -\infty$, is written in the form

$$\hat{P}(s,x) = -\frac{\rho c}{2}\int_{-\infty}^{x}\hat{F}(s,\xi)\,d\xi$$

$$+\left[\frac{1}{c}\int_{-\infty}^{x}J_+(0,\xi)\exp\left(\frac{2s}{c}\xi\right)d\xi + \frac{\rho c}{2}\int_{-\infty}^{x}\hat{F}(s,\xi)\exp\left(\frac{2s}{c}\xi\right)d\xi\right]\exp\left(-\frac{2s}{c}x\right) + a,$$

$$\rho c\hat{u}(s,x) = \frac{\rho c}{2}\int_{-\infty}^{x}\hat{F}(s,\xi)\,d\xi \tag{5}$$

$$+\left[\frac{1}{c}\int_{-\infty}^{x}J_+(0,\xi)\exp\left(\frac{2s}{c}\xi\right)d\xi + \frac{\rho c}{2}\int_{-\infty}^{x}\hat{F}(s,\xi)\exp\left(\frac{2s}{c}\xi\right)d\xi\right]\exp\left(-\frac{2s}{c}x\right) - a.$$

The constant a is found from the requirement for continuity of the Riemann J_- invariant for $x = x_{cr}$. In regions 3*, 4*, etc. (see Fig. 1), the functional dependences of J_- on the coordinates and time are different, and the invariant at each subsequent region is determined only after the solution in the preceding one is found. Let us find the a value within the interval $0 \leqslant T \leqslant 2\tau_{cr}$. In region 3, we have according to (3)

$$J_- = -2\rho c f(-h - ct) = -2\rho c f(-cT). \tag{6}$$

Since the J_- invariant is preserved along the C_- characteristics, relation (6) yields its value in region 3*. Applying the Laplace transform in (6) and equating the relation obtained to the J_- invariant in the fracture region, which follows from (5) for $x = x_{cr}$, we obtain

$$a = \frac{\rho c}{2}\int_{-\infty}^{x_{cr}}\hat{F}(s,\xi)\,d\xi - \rho c\hat{f}(s). \tag{7}$$

Equations (5) and (7) yield solutions in the fracture region for $0 \leqslant T \leqslant 2\tau_{cr}$ in terms of Laplace transforms. Some results can be derive directly from (5), without returning to the originals. For example, using the known property of the Laplace transform [7] $\lim_{s\to\infty}(sG(s)) = G(0)$, we obtain the pressure on the right from the shock along the C_- characteristic in the form

$$P = \rho c(f(2h) - f(0)) + \frac{\rho c}{2}\int_{h}^{h_{cr}}F(0,\xi)\,d\xi, \tag{8}$$

i.e., if the initial fracture velocity is zero, the pressure directly behind the shock varies in the same manner as

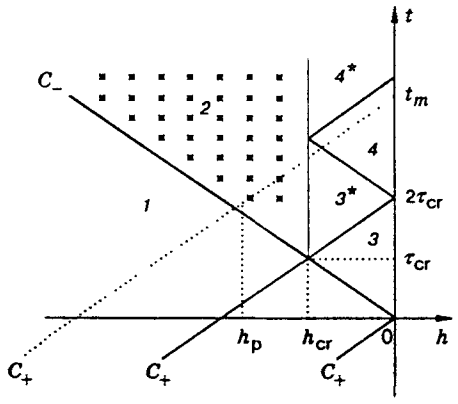

Fig. 1

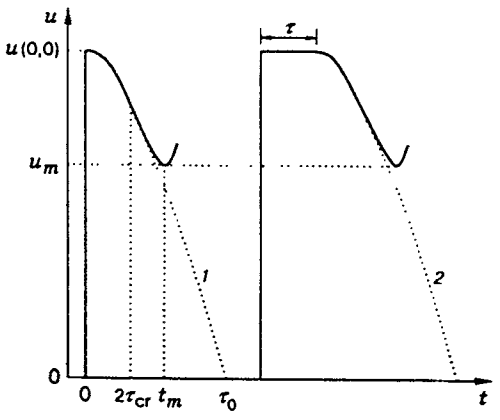

Fig. 2

in the absence of fracture; in particular, with $h \leqslant h_{cr}$ the pressure continues to decrease after the value P_{cr} is attained. Otherwise, Eq. (8) gives the stress-relaxation law: after the onset of fracture the pressure can either continue to decrease or begin to increase, which is determined by the relationship between the fracture velocity and the deformation velocity of the material in the unloading part of the incident pulse [5]. If one assumes that F can be expressed as a function of pressure, Eq. (8) produces the integral equation for determination of P on the right of the shock. This situation was analyzed in detail in [4] where the flow dynamics was studied, with a linear dependence of the fracture velocity on the acting pressure.

We find the velocity of the specimen's free surface. To do this, we use the circumstance that the J_+ invariant is preserved along the C_+ characteristics in the nonfractured part of the specimen. Its value on the free surface equals $\rho c u(0,t)$ and, for $h = h_{cr}$, we have

$$\frac{\hat{J}_+(s, x_{cr})}{\rho c} = \int_{-\infty}^{x_{cr}} \left[\frac{2}{\rho c^2} J_+(0,\xi) + \hat{F}(s,\xi)\right] \exp\left(-\frac{2s}{c}(x_{cr} - \xi)\right) d\xi$$

from the solution obtained in the fracture region.

The general solution (5) contains the constant a, which, as mentioned above, is sequentially found in regions 3^*, 4^*, etc. At the same time, this constant does not enter the relation for the J_+ invariant, and, hence, the free-surface velocity is not dependent on it, and the relation derived below is true for all times. Using the known inversion formulas and the properties of the Laplace transform [7, 8], for the free-surface velocity we find

$$u(0,t) = 2f(-ct) + \Theta(t - 2\tau_{cr}) \int_{-ct/2}^{-c\tau_{cr}} F(t + 2\xi/c, \xi)\, d\xi, \tag{9}$$

where $\Theta(\xi)$ is the Heaviside function. We shall consider the solution obtained with a view for finding the relationship between the free-surface velocity profile and the parameters of fracture kinetics.

Analysis of the Solution. (1) It follows from (9) that the velocity profile repeats the shape of the initial compression pulse at the initial moment of time. At $t = 2\tau_{cr}$, the information on the onset of material fracture reaches the free surface and the velocity turns out to be higher than the velocity that would be in the absence of fracture. Note that at moment $2\tau_{cr}$, as is seen from the above formula, the accelerations remains continuous if the fracture velocity is zero at the initial moment of time. Otherwise a break will be observed at this moment. If definite relations between the incident-pulse parameters and the fracture kinetics are satisfied, a minimum u_m (see Fig. 2) is formed in the velocity profile at moment t_m:

$$\frac{du}{dt} = -2cf'(-ct_m) + \frac{c}{2} F(t_m - 2\tau_{cr}, h_{cr}) - \frac{c^2}{4} \int_0^{t_m - 2\tau_{cr}} F_x\left(\xi, \frac{c}{2}(\xi - t_m)\right) d\xi = 0. \tag{10}$$

Here F_x is the partial derivative of F with respect to x, which is regarded as the function (T, x). Since $f'(-ct_m)$ is the deformation velocity in the incident wave $\rho\dot{v} = \rho\,\partial v/\partial t$ for $h = h_{cr}$ and $t = t_m - \tau_{cr}$, and $F(t_m - 2\tau_{cr}, h_{cr})$ is the fracture velocity $\rho\dot{v}_p = \rho\,\partial v_p/\partial t$ at the same moment, relation (10) can be written as

$$\rho\frac{\partial v_p}{\partial t} - \frac{c}{2}\int_0^{t_m-2\tau_{cr}} F_x\Big(\xi, \frac{c}{2}(\xi - t_m)\Big)\,d\xi = 4\rho\frac{\partial v}{\partial t}. \tag{11}$$

It follows from this, in particular, that if the fracture velocity is constant along the C_- characteristics (i.e., $F_x = 0$), a minimum is formed when $\dot{v}_p = 4\dot{v}$. For the simplest kinetics, this result was derived in [4, 5]. In the general case, this condition is not satisfied quantitatively, but it remains unchanged qualitatively: a minimum on the free-surface velocity profile is formed only under the condition that the fracture velocity reaches a critical value proportional to the deformation velocity in the unloading part of the incident pulse. If, for example, the fracture velocity is increased during the motion along the C_- characteristic in the region of negative x, i.e., $F_x < 0$, a minimum will be observed at the smaller fracture velocities. This case is studied below in more detail using a concrete model as an example.

(2) The spall strength σ^* is determined from the free-surface velocity profile by the difference between the maximum and minimum velocity values:

$$\sigma^* = (1/2)\rho c(u(0,0) - u_m). \tag{12}$$

Clearly, this quantity in the general case depends both on the shape of the loading pulse and on the fracture kinetics. Note that it follows from (11) that σ^* is most affected by the relation between the fracture and deformation velocities in the unloading part of the pulse. Precisely this circumstance allows one to expect to obtain the kinetic information directly from experimental data.

The spall strength is much less sensitive to the shape of the loading pulse in the compression phase. To prove this, we consider two different velocity profiles which coincide in the unloading part of the pulse, but are different in the duration of the "plateau" τ, with constant parameters behind the shock front (see Fig. 2). It is evident that in the second case, fracturing begins later in the deeper layers of the specimen: $\tau_{cr}^{(2)} = \tau_{cr}^{(1)} + \tau/2$ and $h_{cr}^{(2)} = h_{cr}^{(1)} - c\tau/2$. Using relation (10) with allowance for $F^{(2)}(T, \xi - c\tau/2) = F^{(1)}(T, \xi)$, it is easy to see that the moments $t_m^{(1)}$ and $t_m^{(2)}$, which correspond to a minimum on the free-surface velocity profile, are related by the relation $t_m^{(2)} = t_m^{(1)} + \tau$, i.e., the minimum velocity values and, hence, the spall strength remain unvaried.

Our conclusions have so far been fairly general and independent of a concrete fracture kinetics. In what follows, we shall consider a few simple kinetic relations which allow one, nevertheless, to describe the basic experimental results.

(3) Let the incident pulse be shaped like a trapezoid:

$$u(h,t) = f(h - ct) = u_0 + k(h - ct + c\tau)\Theta(h - ct + c\tau). \tag{13}$$

Here u_0 is the maximum value of the mass velocity, k is the constant that characterizes the pulse duration $2h_0$ $[h_0 = -c\tau_0 = -u_0/(2k)]$, and τ is the time during which the velocity is constant and equals u_0. The fracture threshold is reached at the point $\tau_{cr} = -h_{cr}/c = -P_{cr}/(2\rho c^2 k) + \tau/2$.

We consider the fracture kinetics at which the rate of pore growth is a power function of the current pore volume v_p and maximum tensile stresses P_{min} attained in a given particle:

$$\rho\frac{\partial v_p}{\partial t} = \frac{1}{\tau_\mu}\Big(-\frac{P_{min}}{\rho c^2}\Big)^n (\rho v_p)^\alpha, \tag{14}$$

where τ_μ, n, and α are the model constants. As indicated above, since the initial fracture velocity is zero, the maximum tensile stresses which arise to the right of the shock along the C_- characteristic (see Fig. 1) will be the same as if the material would not be fractured: $P_{min} = \rho ck(2h + c\tau)$. With allowance for this circumstance, after integration of relation (14) the function F on the right-hand side of the last equations in

system (1) reduces to the form

$$F(T,x) = \frac{1}{\tau_\mu}\left[-k\left(\frac{2x}{c}+\tau\right)\right]^{n/(1-\alpha)}\left[(1-\alpha)\frac{T}{\tau_\mu}\right]^{\alpha/(1-\alpha)}. \tag{15}$$

Substituting (15) into (9), we find the law of free-surface velocity variation:

$$\frac{u(0,t)}{2u_0} = 1 - \frac{t-\tau}{2\tau_0-\tau} + \frac{c(1-\alpha)^{\alpha/(1-\alpha)}[k(1-\tau)]^{(n+1)/(1-\alpha)}}{4u_0(k\tau_\mu)^{1/(1-\alpha)}} I_{n,\alpha}(t), \tag{16}$$

where $I_{n,\alpha}(t) = \int_0^{1-(2\tau_{cr}-\tau)/(t-\tau)} \xi^{\alpha/(1-\alpha)}(1-\xi)^{n/(1-\alpha)}\,d\xi$.

The integral is equal to zero for a negative value of the upper bound of integration. The time t_m when a minimum is formed in the velocity profile is found from the relation

$$\frac{4(k\tau_\mu)^{1/(1-\alpha)}}{(1-\alpha)^{\alpha/(1-\alpha)}[k(2\tau_{cr}-\tau)]^{(n+\alpha)/(1-\alpha)}}$$

$$= \frac{n+1}{1-\alpha}\left(\frac{t_m-\tau}{2\tau_{cr}-\tau}\right)^{(n+\alpha)/(1-\alpha)} I_{n,\alpha}(t_m) + \frac{2\tau_{cr}-\tau}{t_m-\tau}\left(\frac{t_m-\tau}{2\tau_{cr}-\tau}-1\right)^{\alpha/(1-\alpha)}. \tag{17}$$

Since the difference $2\tau_{cr} - \tau = -P_{cr}/(k\rho c^2)$ is not dependent on τ, it follows from (17) that $t_m - \tau$ is not dependent on τ as well, and, hence, as mentioned above, u_m and σ^* have the same value both for the trapezoidal and triangular pulses. In what follows, without loss of generality we set $\tau = 0$.

Relations (12), (16), and (17) give the dependence of the spall strength on the loading conditions and the parameters of fracture kinetics. This dependence can, however, be considerably simplified if one takes into account the fact that the spall strength exceeds severalfold the tensile strength measured under static conditions [1], i.e., $t_m/(2\tau_{cr}) \geqslant 2$. In addition, we shall show below that, for most metals, the kinetic constant $n \geqslant 4$, i.e., one can consider that $(t_m/(2\tau_{cr}))^n \gg 1$. In this approximation (approximation of large deformation velocities), we obtain

$$kt_m \approx \frac{n+1}{n+\alpha} a_{n,\alpha}(k\tau_\mu)^{1/(n+\alpha)} \quad \left(a_{n,\alpha} = \frac{n+\alpha}{n+1}\left[\frac{4(1-\alpha)^{(1-2\alpha)/(1-\alpha)}}{(n+1)I_{n,\alpha}}\right]^{(1-\alpha)/(n+\alpha)}\right), \tag{18}$$

where the integral $I_{n,\alpha}$ is calculated in the upper integration limit, which is assumed to be equal to unity, and reduces to gamma functions [8]. The spall strength then is a power function of deformation velocity $\rho\dot{v} = k$ and the unloading part of the pulse:

$$\frac{\sigma^*}{\rho c^2} \approx a_{n,\alpha}(\tau_\mu \rho \dot{v})^{1/(n+\alpha)}, \tag{19}$$

where $a_{n,\alpha}$ is a weak function of parameters (of the order of unity). For example, $a_{4,1/2} \cong 1.45$, $a_{5,1/2} \cong 1.38$, $a_{4,2/3} \cong 1.65$, and $a_{5,2/3} \cong 1.56$. Note that although the spall strength in the general case depends on the threshold of fracture onset and $\sigma^* \to -P_{cr}$ for $\dot{v} \to 0$, in the limiting case considered this dependence disappears.

For $\alpha = (m+1)/(m+2)$ $(m = 0, 1, \ldots)$, the integral in (16) is calculated analytically and is of the simplest form for $\alpha = 1/2$. For the spall strength, we here find

$$y = \frac{2n+1}{2n+2}\frac{1}{z}\left[(1+z)^{(2n+2)/(2n+1)} - 1\right], \tag{20}$$

where

$$y = \frac{\sigma^*}{-P_{cr}}; \quad z = \frac{8(2n+1)(\tau_\mu\rho\dot{v})^2}{(-P_{cr}/\rho c^2)^{2n+1}}.$$

Figure 3 shows the dependences $y(z)$ for $\alpha = 1/2$ and various n, which were constructed according to the exact (20) (solid curves) and approximate (19) (dashed curves) formulas. It is seen that the large deformation-velocity approximation is satisfied earlier than was assumed in deriving formula (19). For $n = 4$,

TABLE 1

Material	A, GPa · sec^b	b	Reference	α	n	τ_μ, sec
Kh18N10T stainless steel	0.648	0.11	[9]	1/2	8.59	$1.81 \cdot 10^{-23}$
				2/3	8.42	$0.79 \cdot 10^{-23}$
M2 copper	0.220	0.16	[1]	1/2	5.75	$5.16 \cdot 10^{-19}$
				2/3	5.58	$2.43 \cdot 10^{-19}$
AM g6M aluminum	0.093	0.20	[1]	1/2	4.50	$5.92 \cdot 10^{-16}$
				2/3	4.33	$2.91 \cdot 10^{-16}$
Single-crystal molybdenum	0.144	0.30	[3]	1/2	2.83	$2.70 \cdot 10^{-12}$
				2/3	2.67	$1.44 \cdot 10^{-12}$

the discrepancy does not exceed 6%, beginning with $\sigma^*/(-P_{cr}) = 1.3$, whereas this accuracy is reached already at $\sigma^*/(-P_{cr}) = 1.1$ with an increase in n up to 12. Relation (19) is a good approximation if $\sigma^*/(-P_{cr}) \geqslant 1.4$ even when $n = 3$.

It is known [1, 2] that experimental data are well approximated by relation (19), which is usually written as $\sigma^* = A(\rho\dot{v})^b$. Knowing the constants A and b and specifying the α values, one can find two remaining parameters of fracture kinetics. Table 1 lists the thus calculated parameters of fracture kinetics for two values of α. It is seen that an increase in α from 1/2 to 2/3 leads to a decrease in τ_μ by approximately two times.

Let us consider now what fracture velocities occur in the specimen when a minimum is formed in the free-surface velocity profile. With this in view, we study the variation in $\rho\dot{v}_p$ along the C_+ characteristic passing through the point t_m ($t = t_m + h/c$) (see Fig. 1). It follows from (15) that $\rho\dot{v}_p$ with

$$h_p = -\frac{n}{n+\alpha}\frac{ct_m}{2} \tag{21}$$

reaches the maximum value

$$\frac{(\rho\dot{v}_p)_m}{k} = \left(\frac{n}{n+\alpha}\right)^{n/(1-\alpha)}\left(\frac{\alpha(1-\alpha)}{n+\alpha}\right)^{\alpha/(1-\alpha)}\frac{(kt_m)^{(n+\alpha)/(1-\alpha)}}{(k\tau_\mu)^{1/(1-\alpha)}}. \tag{22}$$

In the approximation (18), we obtain

$$\frac{(\rho\dot{v}_p)_m}{4k} \approx \left(\frac{n}{n+\alpha}\right)^{n/(1-\alpha)}\left(\frac{\alpha}{n+\alpha}\right)^{\alpha/(1-\alpha)}\frac{1-\alpha}{(n+1)I_{n,\alpha}}. \tag{23}$$

Using (23), one an readily show that, for $n \geqslant 4$, the maximum fracture velocity decreases little as n grows, remaining practically constant and equal to its limiting value for $n \to \infty$:

$$\frac{(\rho\dot{v}_p)_m}{4k} \approx \frac{z^z}{e^z\Gamma(1+z)}, \qquad z = \frac{\alpha}{1-\alpha}. \tag{24}$$

Since the constant k equals $\rho\dot{v}$, we again have the statement proved above: a minimum in the free-surface velocity profile is formed when the maximum fracture velocity reaches a critical value which is proportional to the deformation velocity in the unloading part of the pulse: $(\dot{v}_p)_m = \gamma\dot{v}$. Since the fracture velocity increases during the motion along the C_- characteristic deep in the specimen, $\gamma < 4$ and decreases approximately from 2 to 1 with an increase in α from 1/3 to 2/3.

We would like to note some specific features of fracture that are associated with the kinetics (14). First, the spall strength, which is determined by a minimum velocity in the free-surface velocity profile, is smaller in absolute value than the maximum tensile stresses occurring in the specimen at the point $(t_m/2, -ct_m/2)$ (see Fig. 1) by the quantity $\Delta\sigma/\sigma^* = (1-\alpha)/(n+\alpha)$, which can be approximately 10%. This fact is one more argument in favor of the fact that the spall strength characterizes not so much the strength properties of materials under conditions of shock-wave loading as their resistance to fracture under specified conditions.

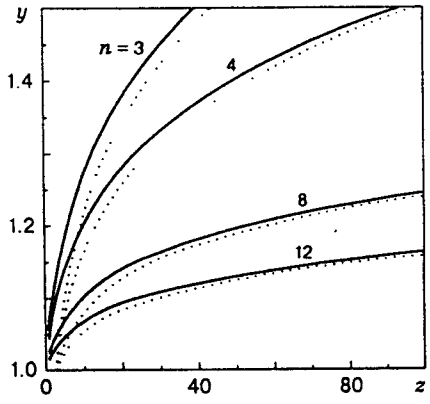

Fig. 3

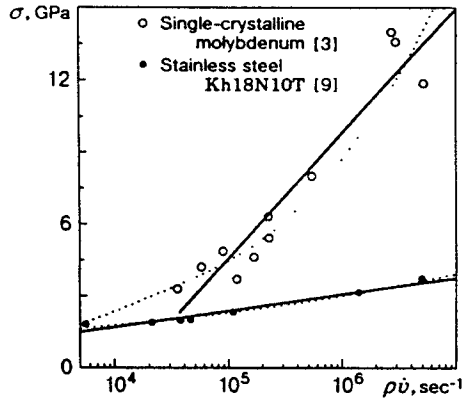

Fig. 4

Second, the model that we have studied is suitable only for description of the initial fracture phase when stresses are tensile and the pore collapse has not yet occurred. With the growth of porosity, the stresses in the fracture region relax and can become positive after a minimum in the free-surface velocity profile is formed. Beginning with this moment, it is necessary to describe the pore collapse, which can be done using the kinetic equation (14) after its modification, for example, after the factor $(-P_{\min})^n$ is replaced by $-P(-P_{\min})^{n-1}$, where P is the current pressure. As shown by Utkin and Kanel [9], this kinetics is suitable for numerical fracture simulation in real materials under spall conditions and describes satisfactorily not only the onset of fracture but also subsequent velocity oscillations in the free-surface velocity profile because of the circulation of waves in a spall plate. We failed to find an analytical solution of the problem in this formulation. However, since the initial and modified kinetics almost coincide at the initial stage of fracture, all the results obtained above, in particular, the dependence of the spall strength on the deformation velocity (19), remain unchanged. This makes it possible to apply the method of determining the kinetic constants from the experimental dependences $\sigma^*(\dot{v})$ in the description of real media if the models used reduce to (14) at the initial stage of fracture.

It is necessary to note that the correspondence of the results derived using the model presented to the experimental results should not be considered as proof of the validity of this form of the kinetic equation. Moreover, the experimental results can be approximated with some accuracy not only by a power dependence of the form (19).

Figure 4 shows the experimental results for single-crystal molybdenum [3] and stainless steel [10] in the coordinates $\sigma^*-\log(\rho\dot{v})$ which are approximated by the relation

$$\sigma^* = A + B\log(\rho\dot{v}). \tag{25}$$

The constants A and B are equal to -24.52 and 5.65 for molybdenum and -0.94 and 0.67 GPa for steel. The dashed curves refer to the approximation by the power function. It is seen that both dependences describe the experimental data with the same accuracy. We shall show that the dependence (25) can be obtained theoretically, with an appropriate choice of the kinetic equation.

(4) As before, we assume that the rate of pore growth depends on the maximum tensile stresses and the current porosity and is of the form

$$\rho\frac{\partial v_p}{\partial t} = \frac{1}{\tau_\mu}\exp\left(-\beta\frac{P_{\min}}{\rho c^2}\right)(\rho v_p)^\alpha, \tag{26}$$

where τ_μ, α, and β are the constants. Defining the function $F(T,x)$ and substituting it into (9), we obtain

the free-surface velocity versus the time:

$$\frac{u(0,t)}{2u_0} = 1 - \frac{t}{2\tau_0} + \frac{c(1-\alpha)^{\alpha/(1-\alpha)}\exp[\beta(1-\alpha)kt]}{4u_0(k\tau_\mu)^{1/(1-\alpha)}} J_{\beta,\alpha}(t) \tag{27}$$

$$\left(J_{\beta,\alpha}(t) = \int_0^{k(t-2\tau_{cr})} \xi^{\alpha/(1-\alpha)}\exp[-\beta(1-\alpha)]\,d\xi\right).$$

Differentiating the velocity with respect to the time and equating it to zero, we find the time of formation of a minimum and then the minimum velocity and the spall strength. If $\exp[-\beta(1-\alpha)k(t_m-2\tau_{cr})] \ll 1$, which corresponds to the approximation of large deformation velocities, we have

$$\frac{\sigma^*}{\rho c^2} \approx \frac{1}{\beta(1-\alpha)} \ln\left[\frac{4\beta^{\alpha/(1-\alpha)}}{e\Gamma(1/(1-\alpha))}\right] + \frac{1}{\beta(1-\alpha)^2} \ln(\tau_\mu \rho \dot{v}), \tag{28}$$

where $\Gamma(x)$ is the gamma function. The relation obtained coincides with relation (25) and, for a given value of α, one can find τ_μ and β using experimental data. For example, if $\alpha = 1/2$, we have $\tau_\mu = 6.6 \cdot 10^{-4}$ sec and $= \beta = 2278$ for steel and $\tau_\mu = 1.8 \cdot 10^{-6}$ sec and $\beta = 439$ for molybdenum.

In concluding, we note that the qualitative character of the dependence of the spall strength on the deformation velocity of both (19) and (28) can also be found directly from the form of the kinetic equations (14) and (26) if the critical spall-pulse formation condition ($\dot{v}_p = \gamma\dot{v}$, where γ is constant) is taken into account and if one assumes that $\sigma^* \sim -P_{min}$. The functional dependence obtained in this case can turn out to be somewhat distorted, because the porosity v_p remains undetermined in this estimation. For example, instead of the dependence (19), we find $\sigma^* \sim (\dot{v})^{1/n}$, i.e., the exponent is not dependent on α. If we take into account that a maximum porosity is attained with $h = (-ct_m/2)n/(n+1)$ and is proportional to σ^*, which can be readily obtained from relation (14) with the use of formulas (18) and (19), the character of the dependence will be correct. But it is obvious that it is impossible to predict that $(v_p)_m \sim \sigma^*$ without the knowledge of an analytical solution.

Thus, we have studied the effect of the fracture kinetics on the formation of a spall pulse within the framework of the acoustic approximation. With an arbitrary fracture kinetics, a minimum in the free-surface velocity profile has been shown to be formed only if the fracture velocity reaches a critical value proportional to the deformation velocity of the material in the unloading part of the pulse. We have proposed an algorithm which allows one to find the kinetic constants if the experimental dependence of the spall strength on the deformation velocity is known.

This work was supported by he International Scientific-Technical Center (Grant No. 124).

REFERENCES

1. A. V. Bushman, G. I. Kanel', A. L. Ni, and V. E. Fortov, *Thermal Physics and the Dynamics of Intense Impulse Actions* [in Russian], Inst. of Chem. Phys., Chernogolovka (1988).
2. G. I. Kanel and V. E. Fortov, "Mechanical properties of condensed media under intense impulse actions," *Usp. Mekh.*, **10**, No. 3, 3–82 (1987).
3. G. I. Kanel, S. V. Razorenov, A. V. Utkin, et al., "Spall strength of molybdenum single crystals," *J. Appl. Phys.*, **74**, No. 12, 7162–7165 (1993).
4. A. V. Utkin, "The effect of the fracture velocity on the dynamics of a shock-loading pulse–body surface interaction," *Prikl. Mekh. Tekh. Fiz.*, No. 6, 82–89 (1992).
5. A. V. Utkin, "The effect of the initial fracture velocity on the formation of a spalling pulse," *Prikl. Mekh. Tekh. Fiz.*, **34**, No. 4, 140–146 (1993).
6. Ya. B. Zel'dovich and Yu. P. Raizer, *Physics of Shock Waves and High-Temperature Hydrodynamic Phenomena* [in Russian], Nauka, Moscow (1973).
7. M. A. Lavrent'ev and B. V. Shabat, *Methods of the Theory of Functions of a Complex Variable* [in Russian], Nauka, Moscow (1973).

8. M. Abramovits and I. Stigan, *Reference Book of Special Functions* [in Russian], Nauka, Moscow (1979).
9. A. V. Utkin and G. I. Kanel, "Estimation of the spall fracture kinetics from the free-surface velocity profiles," in: *APS Topical Conference on Shock Compression of Condensed Matter*, Seattle, USA (1995).
10. K. Baumung, H. J. Bluhm, P. Hoppe, et al., "Hypervelocity launching and impact experiments on the Karlshure light ion facility," *Int. J. Impact Eng.*, **17**, 37–46 (1995).